

https://doi.org/10.1070/QEL17663

Correlation between optical fibre diameter and characteristics of tilted fibre Bragg grating-assisted sensors

K.A. Tomyshev, E.I. Dolzhenko, O.V. Butov

Abstract. **We report the results of a study on the influence of the fibre cladding diameter on the accuracy and resolution of tilted fibre Bragg grating-assisted refractometers. Tilted fibre Bragg gratings are an essential element used to develop high-precision fibre sensors for environmental monitoring. Comparative research was performed using one of comprehensive processing algorithms employing spectral envelope analysis. It was shown that the sensor accuracy decreases with decreasign fibre cladding diameter. At the same time, an increase in the diameter deteriorates the spectral pattern contrast, thus impeding the development of high-efficiency sensor elements.**

Keywords: *tilted fibre Bragg gratings, fibre sensors, signal processing.*

1. Introduction

Great amounts of information are being produced and processed in the modern world. They determine the performance of literally all spheres of life, be it an industrial work, or a medical laboratory, or a residential apartment. The higher the quality of this information, the higher the prediction accuracy and the more efficient the control. New high-precision sensors are being constantly developed to improve the data collection efficiency.

The development of fibre optic sensors is a relatively young independent direction in modern sensorics. A majority of fibre sensors have a number of fundamental advantages in comparison with classical electronic sensors; these advantages include noise immunity, high sensitivity and resolution, and a wide dynamic range [1–4]. A separate group of fibre sensors are the ones with the main sensing element in the form of a fibre Bragg grating (FBG). This grating is a structure with a periodically modulated refractive index, formed in the fibre core (the so-called grooves). A specific feature of this structure is its ability to reflect light only at a certain (Bragg) wavelength, which depends on the grating period and refractive index of the fibre material. Many various FBG-based sensors have been developed or are under development; they include sensors of temperature, strain, pressure, acceleration, etc. [5–10], which can work, in particular, under difficult operating conditions [11–14].

K.A. Tomyshev, E.I. Dolzhenko, O.V. Butov Kotelnikov Institute of Radioengineering and Electronics of Russian Academy of Sciences, ul. Mokhovaya 11-7, 125009 Moscow, Russia;
e-mail: scatterdice@gmail.com

Received 26 October 2021
Kvantovaya Elektronika **51** (12) 1113–1117 (2021)
Translated by Yu.P. Sin'kov

Note that the application range of sensors based on classical FBGs is limited by their sensitivity to only the changes occurring directly in the fibre, be it a change in temperature or a mechanical deformation. However, some problems call for measuring and monitoring environmental parameters, such as composition, refractive index, humidity of a surrounding medium, and presence of chemical or biological impurities in it. In this case the optical signal from a fibre sensor should interact (directly or indirectly) with the environment, which is provided by changing the optical fibre geometry [15, 16] or using cladding modes, which contact the external medium adjacent to the fibre surface [17, 18]. One of the ways to provide this interaction is to form tilted fibre Bragg gratings (TFBGs), that is, gratings in which the groove plane is tilted with respect to the fibre cross section [19–22]. A TFBG partially scatters the fibre-guided radiation into the fibre cladding to form cladding modes. A characteristic transmission spectrum of a tilted grating is a sequence of peaks and dips, where each extremum corresponds to certain cladding modes. In turn, the parameters of these modes depend on the refractive index of the sensor environment, due to which TFBGs can be used to measure environmental parameters [23] (Fig. 1). A characteristic parameter reflecting the sensor response to a change in the refractive index of the environment is the so-called cutoff wavelength. Cladding mode leakage is observed at wavelengths smaller than the cutoff wavelength; this process manifests itself in the TFBG transmission spectrum.

TFBG-based fibre sensors are being actively developed and investigated as applied to many problems, including

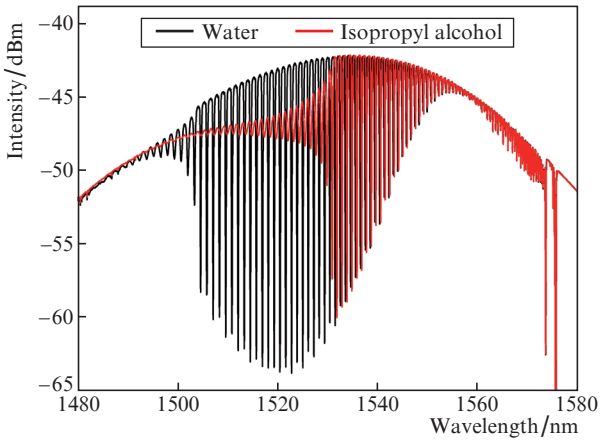

Figure 1. TFBG transmission spectra for liquids with different refractive indices (compositions).

the measurement of the environmental refractive index, atmospheric humidity, and determination of the presence of various impurities in fluids and gaseous atmospheres [20–22, 24–29]. High resolution of TFBG-based sensors, as well as their compactness and integrability into microfluidic systems, make them promising for application in biology and medical diagnostics [30–33]. Note that the specific features of the transmission spectrum of these sensors hinder exact and unambiguous interpretation of their readings. Therefore, an important task is to develop methods and algorithms for processing signals from TFBG-based sensors, which affects directly the measurement accuracy. To date, different methods have been described in the literature, which are based on measuring the amplitude and/or wavelength of individual spectral extrema or their groups [34, 35], plotting and analysing spectral envelopes [23, 36, 37], and studying their Fourier transforms [38].

The TFBG transmission spectrum is formed with allowance for the fibre physical parameters. For example, the repetition rate of the extrema corresponding to the coupling of cladding modes with the core mode depends directly on the cladding diameter. In addition, the latter may affect the contrast of a TFBG spectral pattern, that is, the depth and shape of spectral minima and maxima. In turn, the accuracy of signal processing methods is directly related to the specific features of the grating transmission spectrum. The issue about the relationship between the fibre cladding diameter and the TFBG-based sensor parameters was of interest for researchers earlier as well [39–44]. For example, Chen et al. [39] performed a comparative analysis of the sensitivity of TFBGs inscribed in fibres of different diameters to variations in temperature and mechanical extension. The problem of change in the cladding-mode excitation efficiency for TFBGs with small tilt angles (2° and 5°) during chemical etching of fibre cladding, with allowance for different refractive indices of the environment, was investigated in [40]. In [41], where a TFBG was inscribed, in contrast, at a large angle (81°), it was shown that the sensor sensitivity (determined from the shift of an individual spectral minimum) increases with a decrease in the fibre cladding diameter. The changes in the spectra of gratings inscribed in multimode fibres, caused by decreasing the cladding diameter, were studied in [42]. It was also demonstrated in [43, 44] that the spectral shift of individual extrema in the TFBG spectrum of fibres with a thinner cladding increases, thus improving the sensitivity of these sensors.

In this study we dwell on this issue again, because (with allowance for the new data processing methods based on the complex analysis of spectral pattern) the influence of fibre cladding diameter on the sensor resolution may be rather significant. The high accuracy and resolution provided by the new spectra processing methods impose specific requirements on the quality and content of the spectral pattern and the TFBG properties. As a consequence, the influence of the fibre diameter may be diametrically opposite to that observed when tracing changes in an individual spectral peak (the approach applied, for example, in [43, 44]).

2. Experimental

When studying the parameters of TFBG sensors with different cladding diameters, an experimental grating sample was inscribed in the core of a standard telecommunication fibre SMF-28e. The inscription was performed by exposing the lateral fibre surface to an excimer ArF laser through a phase mask with a period of 1088 nm. The phase mask period was chosen from an available set of wavelengths, proceeding from the convenience of analysing the TFBG spectrum, the main part of which overlapped the emission wavelength range of the superluminescent source used to scan the grating spectrum (1500–1570 nm). The fibre was installed (jointly with the mask) at an angle of 17° to the laser beam wavefront. With allowance for the refractive index of the fibre material, the grating grooves were oriented at an angle of 11.6° to the fibre cross section. The groove tilt angle affects also the shape of the transmission spectrum of a TFBG and the operating range of the refractive index sensor based on it. The choice of angle in our experiments was determined by the necessity of observing the clearly distinguishable cutoff effect in the grating transmission spectrum in the entire range of the refractive indices of the solutions used in experiments. To increase the grating inscribing efficiency, the fibre was preliminarily loaded with hydrogen at a pressure of 100 atm and a temperature of 100 °C for 24 h [30].

To estimate the sensitivity and measurement accuracy of a sensor, the latter was immersed in aqueous solutions of isopropyl alcohol, whose volume concentration changed from 0 (pure water) to 100% (pure alcohol); the corresponding approximate range of variation in the refractive index was from 1.32 to 1.36. For convenience of comparative analysis, the sensor sensitivity was determined in our study as the shift of the cutoff wavelength with an increase in the volume concentration of isopropyl alcohol solution (in nm $\%^{-1}$). It is convenient to use isopropyl alcohol solution as a model liquid, because it is free of processes that can distort experimental results, such as solute precipitation, change in the solution temperature with a change in the solution concentration, etc., which may be typical of, e.g., salt solutions. The signal transmitted through the sensor was measured by a Yokogawa AQ6370D optical spectrum analyser with an actual resolution of 0.017 nm. After a series of measurements, the fibre diameter at the TFBG location site was changed; to this end, the sample was placed in a 10% solution of hydrofluoric acid for 30 min. To estimate the outer cladding diameter after the etching, we used an identical segment of SMF-28e fibre without grating, which was etched together with the sensor; after this procedure the test-fibre diameter was measured by a Vogel 231061 micrometer with an error of 1 μm. According to the measurement results, the decrement in the diameter after each etching iteration turned out to be ~6 μm. After etching in acid the sample was carefully washed with distilled water and dried; then a series measurements in aqueous solutions of isopropyl alcohol with measurement of sensor spectral characteristics was repeated.

Thus, the sensor parameters at different fibre cladding diameters were measured in a series of experiments. The spectral characteristics were processed using the mathematical algorithm described in detail in [23], which implies the plotting of the upper and lower envelopes of the spectrum after its Fourier filtering. The envelopes are smooth curves, fitted by the empirical dependence of the form $A + B\arctan[C(\lambda - \lambda_0)]$ over a set of local spectral extrema (minima and maxima, respectively). The mean values of the spectral coordinates of inflection points (that is, zeros of the second derivatives of envelope functions) are taken to be cutoff wavelength estimates.

3. Results and discussion

Figure 2 shows the spectra of sensors immersed in water, recorded for two different fibre diameters. Note that the amplitude of the spectral peaks increases with a decrease in the cladding diameter, which can be explained by the larger overlap of the field of cladding modes with the core-mode field for a thinner fibre. This circumstance indicates that thinner fibres are preferred for the processing methods based on measuring the amplitudes of individual peaks, because the scale of their variation increases significantly. Indeed, the efficiency of such methods depends directly on the width of the range of variation in amplitude for a separate extremum. At the same time, the number of extrema in the TFBG spectrum increases with an increase in the cladding diameter, which, in turn, should positively affect the accuracy of the algorithms involving analysis over a set of spectral peaks, such as spectral envelope methods [36, 37]. The larger the number of peaks in the spectral pattern, the smaller the error in constructing the envelope (due to the decrease in the statistical weight of the coordinate of each individual spectral peak). In turn, this factor decreases the influence of inhomogeneities and noise (which distort certain spectral portions) on the final processing result.

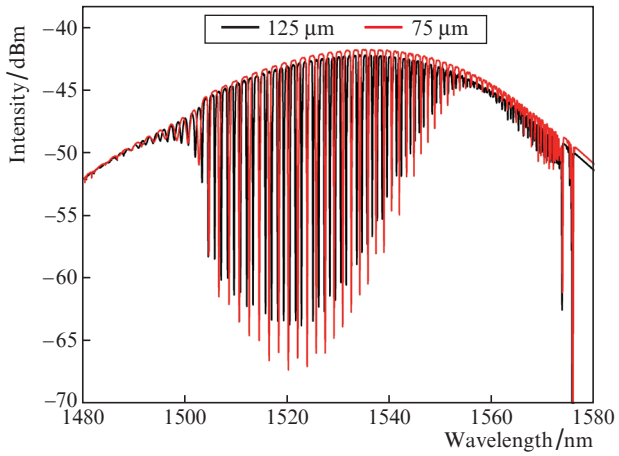

Figure 2. TFBG transmission spectra in water for 75 and 125 μm diameter fibres.

The results of processing the spectral data obtained using solutions with different isopropyl alcohol concentrations are presented for a sensor 125 μm in diameter in Fig. 3. It can be seen that the dependence is essentially nonlinear. This behaviour is explained by the nonlinear dependence of the refractive index of isopropyl alcohol solution on its concentration [45, 46]. In the first approximation this dependence can be fitted by a third-order polynomial in the form

$$\lambda_c = \lambda_0 + AC^3 + BC^2 + DC,$$

where λ_c is the cutoff wavelength and λ_0, A, B, and D are polynomial coefficients.

Similar results were obtained for all other fibre diameters. Obviously, such sensor parameters as accuracy and resolution are interrelated via the calibration coefficients. The resolution (and, correspondingly, potential accuracy) is generally considered to be the value of triple standard deviation of sensor readings from the real measured value. In our case the parameter allowing one to obtain a relative estimate of the sensor accuracy is the standard deviation of the measured cutoff wavelength from the fitting curve. The smaller this parameter, the higher the resolution and potential accuracy of the sensor are.

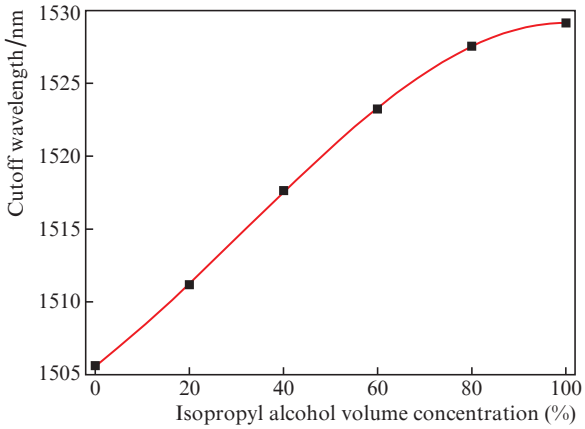

Figure 3. Cutoff wavelength at different isopropyl alcohol concentrations for a 125 μm diameter fibre.

A comparison of the results of this processing did not reveal any explicit changes in the sensor sensitivity with a change in the fibre diameter (Table 1). At the same time, one can observe an unambiguous correlation between the fitting accuracy and, as a consequence, between the standard deviation of experimental points and the cladding diameter. The calculation results were used to construct a dependence of the standard deviation on the sensor diameter (Fig. 4). It can be seen in the figure that the standard deviation increases with a decrease in the fibre diameter, which indicates deterioration of the sensor resolution. As was noted above, the results of this experiment have some physical meaning. Indeed, the number of peaks in the TFBG spectrum decreases with a decrease in the cladding diameter. Due to this, the statistical weight of the error in determining the spectral coordinate of each separate peak increases, and specifically this circumstance explains the deterioration of the sensor resolution on the whole. Vice versa, an increase in the cladding diameter naturally improves the accuracy of the methods based on con-

Table 1. Average sensor sensitivity χ on different portions of the fitting curve and the standard deviation of experimental points from the curve for different fibre diameters d.

d/μm	χ/nm %$^{-1}$ in concentration ranges		Standard deviation/nm
	0–10%	40%–60%	
125	0.251	0.291	0.010
117	0.290	0.285	0.020
111	0.275	0.292	0.051
106	0.272	0.283	0.063
100	0.285	0.290	0.071
94	0.247	0.292	0.083
87	0.238	0.287	0.118

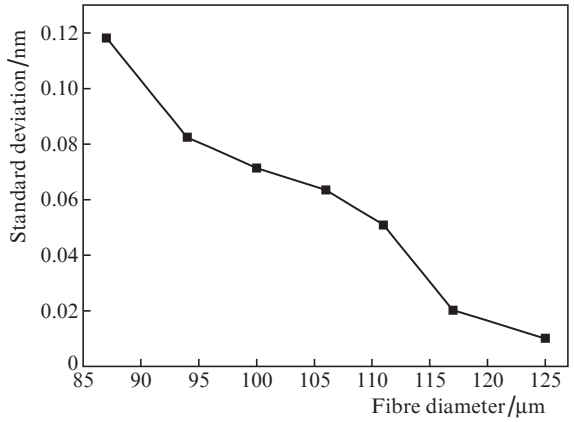

Figure 4. Change in the standard deviation of experimental points from the fitting curve with an increase in the fibre diameter.

structing envelopes, which allows one to increase the operation accuracy of TFBG-based sensors.

Note that, with all advantages of designing TFBG-based sensors in fibres with a thickened cladding, one should not forget that the spectral peak amplitude decreases with an increase in the cladding diameter. This fact may lead to technological difficulties when inscribing efficient tilted Bragg gratings and applying them as high-precision sensors. The spectral peak amplitude for such a grating may be much lower than the desired one, a factor that may affect the processing accuracy.

Thus, an optimal value of sensor diameter can be found for each TFBG-based measurement system, which would provide an amplitude of spectral peaks sufficient for correct measurements and their fairly high spectral density, affecting the sensor resolution. However, this optimal value depends, on the one hand, on the structure of the system and equipment in use and the technique of spectrum analysis; on the other hand, it is determined by the technological possibilities of TFBG manufacturer.

4. Conclusions

The influence of fibre diameter on the characteristics of TFBG-assisted refractive index sensors was investigated. Spectral data were processed using the envelope analysis method, which takes into account the contribution of multiple spectral peaks and provides a high resolution for this type of sensors. According to the data obtained, the measurement accuracy steadily decreases with a decrease in the fibre cladding diameter. An increase in the cladding diameter, in contrast, should improve the resolution of such sensors, provided that the processing algorithms are based on complex spectral analysis (which takes into consideration many spectral peaks); the sensor sensitivity does not exhibit any significant changes under these conditions. However, the efficient inscription of tilted Bragg gratings in fibres with a thicker cladding is a more difficult task, which may be a hindrance when designing sensor elements on their basis. Obviously, one can find an optimal value of the sensor cladding diameter, which is determined by both the possibilities of the spectral equipment applied in the measurement system and the technological potential of the TFBG manufacturer.

Acknowledgements. This work was supported by the Russian Foundation for Basic Research (Grant No. 20-07-00467).

References

1. Zhou W., Zhou Y., Albert J. *Laser Photon. Rev.*, **11** (1), 1600157 (2017).
2. Alwis L., Sun T., Grattan K.T.V. *Measurement*, **46** (10), 4052 (2013).
3. Ascorbe J. et al. *Sensors*, **17** (4), 893 (2017).
4. Lydon M. et al. *IEEE Sens. J.*, **14** (12), 4284 (2014).
5. Kashyap R. *Fiber Bragg Gratings* (Montreal: Academic Press, 2009).
6. Allil R.C.D.A.S.B., Werneck M.M., de Nazaré F.V.B. *Fiber Bragg Gratings: Theory, Fabrication, and Applications* (Bellingham, Washington: SPIE PRESS, 2017).
7. Butov O.V., Bazakutsa A.P., Chamorovskiy Y.K., Fedorov A.N., Shevtsov I.A. *Sensors*, **19** (19), 4228 (2019).
8. Basumallick N., Chatterjee I., Biswas P., Dasgupta K., Bandyopadhyay S. *Sens. Actuat. A*, **173** (1), 108 (2012).
9. Zhuo Z.C., Ham B.S. *Opt. Fiber Technol.*, **15** (5), 442 (2009).
10. Butov O.V. et al. *Versatile in-Fiber Bragg Grating Pressure Sensor for Oil and Gas Industry in Optical Fiber Sensors* (Cancun: OSA Techn. Digest, 2006).
11. Butov O.V., Dianov E.M., Golant K.M. *Meas. Sci. Technol.*, **17** (5), 975 (2006).
12. Mihailov S.J. *Sensors*, **12** (2), 1898 (2012).
13. Butov O.V., Chamorovskii Y.K., Golant K.M., Shevtsov I.A., Fedorov A.N. *Proc. SPIE*, **9157**, 91570X (2014).
14. Butov O.V., Chamorovskiy Y.K., Bazakutsa A.P., Fedorov A.N., Shevtsov I.A. *Optical Fiber Sensor for Deformation Monitoring of Fuel Channels in Industrial Nuclear Reactors in Optical Fiber Sensors* (Lausanne: OSA Techn. Digest, 2018).
15. Korposh S., James S.W., Lee S.W., Tatam R.P. *Sensors*, **19** (10), 2294 (2019).
16. Riza M.A., Go Y.I., Harun S.W., Maier R.R.J. *IEEE Sens. J.*, **20** (14), 7614 (2020).
17. Ivanov O.V., Nikitov S.A., Gulyaev Yu.V. *Usp. Fiz. Nauk*, **176** (2), 175 (2006) [*Phys. Usp.*, **49** (2), 167 (2006)].
18. Erdogan T. *J. Opt. Soc. Am. A*, **14** (8), 1760 (1997).
19. Butov O.V., Tomyshev K.A., Nechepurenko L.A., Dorofeenko A.V., Nikitov S.A. *Usp. Fiz. Nauk*, **65** (2022) (in press) [*Phys. Usp.*, **65** (2022) (in press)].
20. Guo T., Liu F., Guan B.O., Albert J. *Opt. Laser Technol.*, **78**, 19 (2016).
21. Albert J., Shao L.Y., Caucheteur C. *Laser Photonics Rev.*, **7** (1), 83 (2013).
22. Dong X., Zhang H., Liu B., Miao Y. *Photonics Sens.*, **1** (1), 6 (2011).
23. Tomyshev K.A., Manuilovich E.S., Tazhetdinova D.K., Dolzhenko E.I., Butov O.V. *Sens. Actuators A*, **308**, 112016 (2020).
24. Zhao Y., Wang Q.I., Huang H.J. *Optoelectron. Adv. Mater.*, **12**, 2343 (2010).
25. Caucheteur C., Mégret P. *IEEE Photonics Technol. Lett.*, **17** (12), 2703 (2005).
26. Voisin V., Caucheteur C., Mégret P., Albert J. *Appl. Opt.*, **50** (22), 4257 (2011).
27. Dolzhenko E.I., Tomyshev K., Butov O.V. *Phys. Status Sol. RRL*, **14** (12), 2000435 (2020).
28. Tomyshev K.A., Tazhetdinova D.K., Manuilovich E.S., Butov O.V. *Phys. Status Sol. A*, **216** (3), 1800541 (2018).
29. Yu J., Wu Z., Yang X., Han X. *Sensors*, **18** (12), 4478 (2018).
30. Tomyshev K.A., Tazhetdinova D.K., Manuilovich E.S., Butov O.V. *J. Appl. Phys.*, **124** (11), 113106 (2018).
31. Rich R.L., Myszka D.G. *J. Mol. Recognit.*, **18** (6), 431 (2005).
32. Han L., Guo T., Xie C., Xu P., Lao J., Zhang X., Xu J., Chen X., Huang Y., Liang X., Mao W., Guan B.O. *J. Lightwave Technol.*, **35** (16), 3360 (2017).
33. Marquez-Cruz V., Albert J. *J. Lightwave Technol.*, **33** (16), 3363 (2015).
34. Pham X., Si J., Chen T., Wang R., Yan L., Cao H., Hou X. *J. Appl. Phys.*, **123** (17), 174501 (2018).

35. Chan C.F., Chen C., Jafari A., Laronche A., Thomson D.J., Albert J. *Appl. Opt.*, **46** (7), 1142 (2007).
36. Manuylovich E., Tomyshev K., Butov O.V. *Sensors*, **19** (19), 4245 (2019).
37. Lobry M., Fasseaux H., Loyez M., Chah K., Goormaghtigh E., Wattiez R., Chiavaioli F., Caucheteur C. *J. Lightwave Technol.*, **1** (2021) (in press).
38. Udos W., Lim K.S., Tan C.L., Ismail M.N.S.M., Ooi C.W., Zakaria R., Ahmad H. *Optik*, **219**, 164970 (2020).
39. Chen C., Caucheteur C., Mégret P., Albert J. *Meas. Sci. Technol.*, **18** (10), 3117 (2007).
40. Caucheteur C., Chah K., Lhomme F., Debliquy M., Lahem D., Blondel M., Megret P., in *Proc. of 2005 IEEE/LEOS Workshop on Fibres and Optical Passive Components* (Palermo: IEEE, 2005) p 234.
41. Lu H., Luo B., Shi S., Zhao M., Lu J., Ye L., Zhong N.B., Tang B., Wang X., Wang Y. *Appl. Opt.*, **57** (10), 2590 (2018).
42. Chen X., Zhou K., Zhang L., Bennion I. *IEEE Photonics Technol. Lett.*, **17** (4), 864 (2005).
43. Miao Y., Liu B., Zhao Q., in *Proc. of the 2008 International Conference on Advanced Infocomm Technology* (Shenzhen: Association for Computing Machinery, 2008).
44. Miao Y., Liu B., Tian S., Zhao Q. *Proc. SPIE*, **7134**, 71343W (2008).
45. Chu K.Y., Thompson A.R. *J. Chem. Eng. Data.*, **7** (3), 358 (1962).
46. Edward W.W. *International Critical Tables* (New York: McGraw-Hill, 1933).